論文

분자동력학 해석을 이용한 인덴테이션시 실리콘 내부의 결함구조에 관한 연구

트란 딘 롱[*], 유용문[**], 강우종[***], 전성식[*+]

A molecular dynamics simulation on the defect structure in silicon under indentation

Long Trandinh[*], Yong-Moon Ryu[**], Woo-Jong Kang[***] and Seong Sik Cheon[*+]

ABSTRACT

In this paper, the symmetric axis parameter method, which was proposed to identify defects, dislocations and stacking fault, with perfect structures in the zinc-blende materials, was introduced as a way to distinguish between elastic and plastic deformation. LAMMPS, a molecular dynamics programme of Sandia National Laboratories, was used to perform nanoindentation simulation on silicon, a zinc-blende material. Defects in silicon (111) under spherical indentation showed the threefold pattern and the slip system in the form of ring crack. Also simulation results show good agreement with experimental results and existing theoretical analyses.

초 록

본 논문에서는 zinc blende계열의 결정구조를 갖는 실리콘 내부의 결함을 분석할 수 있는 대칭축 파라메터(Symmetric axis parameter)방법을 이용하여, 탄성 및 소성 변형을 구별하는 방법을 제시하였다. 분자 동력학 해석프로그램인 LAMMPS를 사용하여, 실리콘에 대한 나노인덴테이션 해석을 수행하였다. 구형 인덴터 아래에 발생한 실리콘내부의 결함은 ring crack에서의 threefold 무늬와 전위발생경로를 보여주었다. 또한, 해석결과는 기존의 이론이나, 실험결과와도 일치하는 것을 확인하였다.

Key Words : 대칭축 파라메터(Symmetric axis parameter), 원자단위 해석(Atomistic simulation), 나노인덴테이션(Nanoindentation), 인덴테이션 결함(Indented defect)

1. Introduction

Defects such as dislocation and stacking fault are nucleated in materials during deformation process. The defects move inside materials under external load to initiate the plastic deformation. The motion is damped by grain boundary in poly-crystal materials or by interface in layered materials as well as composite materials and resulted in pile-up of dislocations [1]. Therefore, the grain boundary and the interface are considered as obstacles of initiation of plastic deformation, the more there are obstacles the more difficult to initiate plastic zones. Consequently, yield stress is inversely proportional to the square of grain size (the Hall-Petch relation) [2,3]. Therefore, the reactions of defects have strong effect on mechanical properties of materials.

Defects are nucleated and driven by external load such as indentation load, their motion initiates plastic deformation as mentioned above. The defects nucleated by indentation are influenced by environment conditions, point defect and temperature [4,5], or applied conditions such as the load, rate

접수: 2010년 11월 9일, 수정: 2011년 2월 25일, 게재승인: 2011년 3월 22일
* Division of Mechanical and Automotive Engineering, Kongju National University
** Korea Automotive Technology Institute
*** School of Mechanical and Automotive Engineering, Kyungil University
*+ Corresponding author, Division of Mechanical and Automotive Engineering, Kongju National University(E-mail:sscheon@kongju.ac.kr)

and the indenter shape [6,7] [8-13]. A simulation study on defects in silicon such as quasistatic density functional theory was carried on by Perez et al. [14]. They showed the formation of interstitial defects and extrusion in silicon under nanoindentation. Kallmann et al. [15] carried out the molecular dynamics simulations of nanoindentation on silicon using the Stillinger-Weber potential [16] and reported appearance of an amorphous phase beneath the indenter. However, there is still lacking of detailed defect structures for understanding plastic deformation during the indentation on the silicon thin film.

Analysis of defect reactions based on images is a common method to explore plastic deformation process. In order to obtain these images in simulation the defect parts must be distinguished from the perfect parts. Theoretically, defects can be identified from the elastic region of material bases on the electron density technique [17] and the potential energy method [18]. The easier and effective method, centrosymmetry parameter, was proposed by Kelchner et al [19]. Defect configurations are distinguished from perfect configurations and classified into stacking fault, partial dislocation or free surface depending on their centrosymmetry property. Unfortunately, this method is only effective with the centro-symmetry materials such as face centred cubic (FCC) or body centred cubic (BCC) materials.

For the reasons, the symmetric axis parameter was proposed to identify defects in the materials with crystal structure of zinc-blende in this article. Dislocation and stacking fault configurations are distinguished from perfect configurations by symmetric attribute of atoms along four bonds connected to an atom. Defects in silicon (111) under spherical indentation show the threefold pattern, the slip system in the form of ring crack and good agreement with experimental results and theoretical analyses.

2. Symmetric axis parameter

The zinc-blende lattice corresponds to two interpenetrating FCC lattices, one of which is placed at (¼ ¼ ¼) with respect to the other [20]. The layer structure contains (111) planes in the sequence AaBbCc as shown in Fig. 1. Each atom on the bond Bb connected to other three atoms and their vectors aB and Cb are symmetric through the “axis” Bb. In general, directions and lengths of those bonds are changed when deformation occurs. However, those bonds are still symmetric if the lattice is undergoing homogeneously elastic deformation. Apparently, these bond structures are no longer symmetric when any defect is initiated by plastic deformations. Therefore, the symmetric axis parameter is proposed to recognise the defects in materials with zinc-blende crystal structure. The symmetric axis parameter is defined by

$$P_i = \sum_{j=1,4} \sum_{k=1,3} \left| R_k^{(i)} + R_k^{(j)} \right|^2 \quad (1)$$

where $R^{(i)}$ and $R^{(j)}$ are vectors or bonds corresponding to three nearest neighbours of atoms i and j, respectively. The square of vector summation is computed for all bonds connected to the arbitrarily selected atom i.

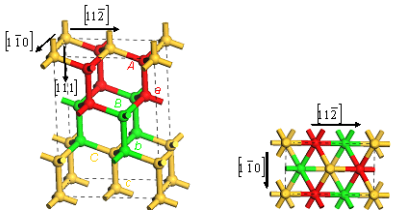

(a) (b)

Fig. 1 Zinc-blende lattice, (a) (111) lattice structure and (b) the projection in direction, the *aB* bonds are axis symmetric to the *bC* bonds and the Ac bonds.

For the case of the Silicon with lattice constant of 5.43 Å [21], the symmetric axis parameter is zero if the atoms are in a perfect lattice. When it contains a stacking fault, the parameter changed to 16.58 Å2 and 4.44 Å2 for atoms in dislocation. These values were calculated based on the fixed bond length condition in the vicinity of the defects which includes the glide set, the shuffle set of 60° perfect dislocations, partial dislocations and a stacking fault [20]. The defects were introduced in a single crystalline silicon model to demonstrate the efficiency of the symmetric axis parameter. First, a perfect single crystalline silicon (30.7 Å ×99.7 Å ×103.4 Å) with three directions of $[1\bar{1}0]$, $[11\bar{2}]$ and $[111]$ was prepared as depicted in Fig 2 (a). Second, atoms and bonds, which were randomly chosen by two dotted rectangles in Fig. 2(a), were removed and the model was rearranged. Consequently, a dislocation couple and Shockley partial dislocations, which bounded a stacking fault, were created in the model as shown in Fig 2(b).

Last, this model was relaxed under the application of Tersoff potential [22] for 10 ps (picoseconds) at zero degrees Kelvin with the three dimensional periodic conditions by the atomistic simulation programme (LAMMPS) [23]. In the mean time, the symmetric axis parameters for all atoms were computed at every 2 ps.

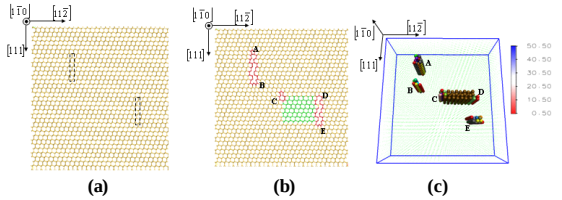

Fig. 2 Single crystal silicon film, (a) perfect structure, the dotted rectangles mark the cut regions, (b) the structure with defects after atoms and bonds rearrangement, the glide set dislocation at A, the shuffle sets at B, E, the partial dislocations bounded the stacking fault at C, D, (c) the relaxed structure with magnifying atoms in defects view.

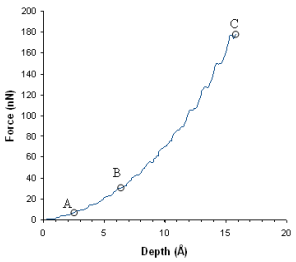

Fig. 3 The force vs depth curve of silicon (111) during indentation and circles mark the points where the lattice structure is changed, homogeneous dislocation nucleation at the A, the partial dislocation nucleation at the B and analysis of dislocation glide at the C.

In Fig. 2(c), the relaxed model was plotted with atoms, whose colours were dependent on the value of the symmetric axis parameter, but there is no feature for distinguishing between glide set and shuffle set dislocation. The figure shows that the symmetric axis parameter method successfully identifies defects in the prepared model, therefore, this method can be applied to find the defect region in the zinc-blende structure.

3. Indentation

A model for the single crystal thin film of silicon with the crystal directions of $[1\bar{1}0]$, $[11\bar{2}]$ and $[111]$, and dimension 106.32×107.44×106.64 Å was prepared for indentation simulation. The model occupies the periodic boundary condition for side directions and the fixed condition for several layers of atoms at the bottom in the $[111]$ direction. Tersoff potential was employed for describing the interaction between two silicon atoms. Indentation on the top free surface of the film was carried out by the rigid 20 Å-radius spherical indenter with 2 m/s constant speed. The interaction between the indenter

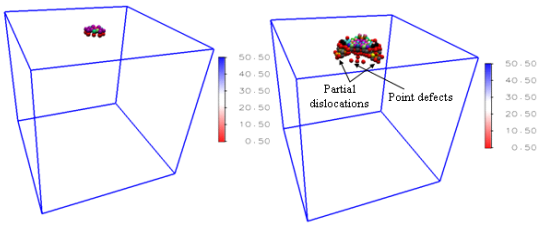

Fig. 4 Defect structures, (a) homogeneous dislocation nucleation at the 2.6 Å indentation depth, (b) partial dislocation nucleation at the 6.3 Å indentation depth.

and atoms was described by the potential [19] and the force constant of 10 eV/Å3 was adopted from Lilleodden et al. [24]. The model was relaxed for 10 ps for equilibrium prior to indentation and the full process was carried out at zero degrees Kelvin.

The force versus depth curve during the indentation is shown in Fig. 3, where, a homogeneous nucleation of dislocation occurs at point A, the partial dislocation nucleation happens at point B and propagation of stacking faults are conspicuous at point C. The fluctuations in the indentation curve imply the elastic stress under the indenter is partially relieved by cracks in film part [9].

The defect structure at each stage of A and B is illustrated in Fig. 4. The initial dislocations appear underneath the indenter and emit from the top surface of the film along with (111) plane. These dislocations are developed with ongoing indentation and the partial dislocations nucleate on the three slip plane family (111). Also, point defects, which are clearly separated from the main defect region, are formed by change of the lattice structure (from zinc-blende to body centred cubic) [10].

The zinc-blende lattice corresponds to two interpenetrating FCC lattices as mentioned above. Thus the slip systems as similar to those of FCC crystal systems, (111) slip planes and [110] slip directions. Perfect dislocations are mainly formed along [110] direction and incline a 60° angle of to their Burgers vectors. A perfect dislocation can dissociate into 2 partial dislocations, 30° and 90° dislocations, which bound a stacking fault, and this rule was concluded in Frank's tetrahedron [27]. For the case of indentation on silicon (111) the slip induces dislocation reactions and curved end of slip lines along with [110] directions complete the ring slip [9]. Three stacking fault bounded by the half loops of partial dislocation glides in three slip planes (111) of the Frank's tetrahedron to form the threefold pattern as shown in Fig. 5. The half loops of partial dislocation

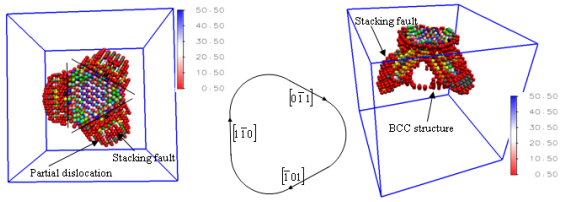

Fig. 5 Defect structure at the indentation depth of 15.9 Å, the ring slip include three [110] slip lines on the free surface and three stacking faults bounded by partial dislocations in [111] slip planes, (a) the top view, (b) the ring slip, (c) the 3D view.

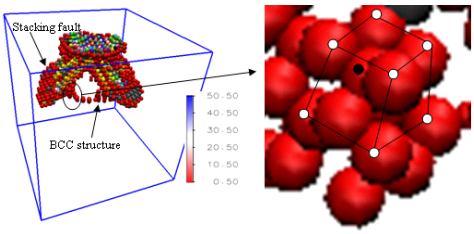

Fig. 6 Defect structure at the indentation depth of 15.9 Å (a), the magnifying of the point defect structure (b), the atoms at corners were marked by opened circles and the central one was by a solid circle.

ended at the free surface by the emission of slip lines. The result shows the good agreement with the results which was experimentally and theoretically performed by Gerbig et al [26].

Furthermore, the substance of the forming defects under indentation by the changing crystal structure of defects from the perfect is phase transformation. For instance, the stacking fault in silicon is formed by transforming from zinc-blende structure of the perfect into hexagonal close-packed structure of the defect. The transmission electron microscopy image of silicon under indentation showed the formation of amorphous phase under indenter and below that the BCC particles were nucleated separately from the amorphous [8-13]. Defect structure at indentation depth of 15.9 Å in Fig. 6 shows point defects located separately from the main defect zone, analysis of crystal structure proved the BCC structure of point defects the same as formation BCC particles [11].

4. Conclusions

The indented plastic deformation of the single crystalline silicon thin film was investigated by atomistic simulation at zero degrees Kelvin. The symmetric axis parameter is proposed to identify the defect region in the zinc-blende structure. It was found that this method successfully separates the perfect dislocations, the partial dislocations and the stacking fault from perfect structure. However, it can not distinguish between glide set and shuffle set dislocations.

The given defect structures, which include dislocation propagation on slip plane and slip direction, reasonably match with the published results about silicon indentation. This work gives a way to distinguish between elastic and plastic deformation and remains a method to study the plastic deformation for zinc-blende materials.

Acknowledgements

This study was supported by the National Research Foundation of Korea under the grant number of 2009-0075193.

References

1) L. Trandinh, A.K. Kim, S.S. Cheon, “Nanoindentation behaviours of silver film/copper substrate,” Journal of Korean Society for composite materials, Vol. 22, 2009, pp. 9-17.
2) E.O. Hall, “The deformation and ageing of mild steel: m. Discussion of results,” Proceedings of the Physical Society B 64, 1951, 747-753.
3) N.J. Petch, “The cleavage strength of polycrystals,” Journal of the Iron and Steel Institute, Vol. 174, 1953, pp. 25-8.
4) V.V. Bulatov, S. Yip, A.S. Argon, “Atomic modes of dislocation mobility in silicon,” Philosophical Magazine A Vol. 72, 1995, pp. 453-496.
5) A. George, S. Yip, “Preface to the Viewpoint Set on: - Dislocation mobility in silicon,” Scripta Materialia, Vol. 45 2001, pp. 1233-1238.
6) K. Higashida, T. Kawamura, T. Morikawa, Y. Miura, N. Narita, “HVEM observation of crack tip dislocations in silicon crystals,” Materials Science and Engineering A Vol. 319-321, 2001, pp. 683-686.
7) K. Asaoka, T. Umeda, S. Arai, H. Saka, “Direct evidence for shuffle dislocations in Si activated,” Materials Science and Engineering A, Vol. 400-401, 2001, pp. 93-96.
8) G.S. Smith, E.B. Tadmor, N. Bernstein, E. Kaxiras, “Multiscale simulations of silicon nanoindentation,” Acta Materialia, Vol. 49, 2001, pp. 4089-4101.

9) R.W. Armstrong, A.W. Ruff, H. Shin, “Elastic, plastic and cracking indentation behavior of silicon crystals,” Materials Science and Engineering A, Vol. 209, 1996, pp. 91-96.
10) T. Vodenitcharova, L.C. Zhang, “A mechanics prediction of the behaviour of mono-crystalline silicon under nano-indentation,” International Journal of Solids and Structures, Vol. 40, 2003, pp. 2989–2998.
11) I. Zarudi, L.C. Zhang, “Structure changes in mono -crystalline silicon subjected to indentation - experimental findings,” Tribology International, Vol. 32, 1999, pp. 701-712.
12) E.R. Weppelmann, J.S. Field, M.V. Swain, “Observation, analysis, and simulation of the hysteresis of silicon using ultra-micro-indentation with spherical indenters,” Journal of Materials Research, Vol. 8, 1993, pp. 830-840.
13) J. Jang, M.J. Lance, S. Wen, T.Y. Tsui, G.M. Pharr, “Indentation-induced phase transformations in silicon: influences of load, rate and indenter angle on the transformation behavior,” Acta Materialia, Vol. 53 (2005) 1759-1770.
14) R. Perez, M.C. Payne, A.D. Simpson, “First principles simulations of Silicon nanoindentation,” Physical Review Letters, Vol. 75, 1995. pp. 4748-4754.
15) J.S. Kallmann, W.G. Hoover, C.G. Hoover, A.J. De Groot, S.M. Lee, F. Wooten “Molecular dynamics of silicon indentation,” Physical Review B, Vol. 47, 1993, pp. 7705-7713.
16) F.H. Stillinger, T.A. Weber, “Computer simulation of local order in condensed phases of silicon,” Physical Review B, Vol. 31, 1985, pp. 5262-5271.
17) V. Gavini, K. Bhattacharya, M. Ortiz, “Vacancy clustering and prismatic dislocation loop formation in aluminum,” Physical Review B, Vol. 76, 2007, 180101.
18) A.F. Bower, Applied Mechanics of Solids, 1st ed., CRC Press 2009, Boca Raton.
19) C. Kelchner, S.J. Plimpton, J.C Hamilton, “Dislocation nucleation and defect structure during surface indentation,” Physical Review B, Vol. 58, 1998, pp. 11085-11088.
20) J.P. Hirth, J. Lothe, Theory of Dislocations, 2nd ed., Wiley Interscience, New York, 1982.
21) W.C. O'Mara, R.B. Herring, L.P. Hunt, Handbook of Semiconductor Silicon Technology, Noyes, New Jersey, 1990.
22) J. Tersoff, “New empirical approach for the structure and energy of covalent systems,” Physical Review B, Vol. 37, 1988, pp. 6991-7000.
23) S.J. Plimpton, B.A. Hendrickson, In: Broughton J, Bristowe P, Newsam J, (editors). Materials theory and modelling, MRS Proceedings, Vol. 291, 1993, Pittsburg, pp. 37.
24) E.T. Lilleodden, J.A. Zimmerman, S.M Foiles, W.D Nix, “Atomistic simulations of elastic deformation and dislocation nucleation during nanoindentation,” Journal of the Mechanics and Physics of solids, Vol. 51, 2003, pp. 901-920.
25) A. Hull, D.J. Bacon, Introduction to Dislocations, 4th ed., Butterworth-Heinemann, Oxford, 2001, Chap.4.
26) Y.B Gerbig, S.J. Stranick, R.F. Cook, “Point defect interaction with dislocations in silicon,” Scripta Materialia, Vol. 63, 2010, pp. 512-515.